Comparison of Shuttle Orbiter Surface Pressures with Wind Tunnel and Theoretical Predictions

P. F. Bradley,* P. M. Siemers III,† and K. J. Weilmuenster†
NASA Langley Research Center, Hampton, Virginia

Surface pressure information obtained from measurements in the forward fuselage region of the Space Shuttle Orbiter during its re-entry through the atmosphere can be used in various aerodynamic calculations. These pressure data are part of the overall flight data system on the Orbiter and are designated Development Flight Instrumentation (DFI). In order that ground-based pressure distribution prediction techniques may be verified by the actual performance of the Orbiter in flight, a comparison between this flight pressure data and both wind tunnel and computational data is presented. An analysis of the Orbiter's pressure data system, including the transducers, their behavior, and calibration, is also presented. This analysis provides the opportunity for an error assessment calculation for the flight data and an explanation of any differences between flight- and ground-based data.

Nomenclature

BETQ	= freestream dynamic pressure calculated by BET, Pa
NAVQ	= freestream dynamic pressure calculated by navigation solution based on wind tunnel data book, Pa
P	= pressure, Pa
ΔP	= error calculation in pressure reading, Pa
Q	= freestream dynamic pressure, Pa
SEADSQ	= freestream dynamic pressure calculated using SEADS algorithm, Pa
V	= velocity, m/s
X/L	= nondimensional length
X,Z	= Orbiter coordinates, in.
α	= angle of attack, deg
β	= angle of sideslip, deg
ρ	= density, kg/m^3
σ	= standard deviation
θ	= incidence angle

Subscripts

fs	= full scale
t_2	= total conditions behind shock
∞	= freestream conditions

Introduction

THE Orbiter Flight Test (OFT) Program, flights 1 through 4, was designed to demonstrate and certify the Space Transportation System (STS) as an operational vehicle. To accomplish the required performance verification and certification of the STS, various types of instrumentation have been installed throughout the vehicle. This instrumentation, designated Development Flight Instrumentation (DFI), was installed to determine the overall aerodynamic and aerothermodynamic performance to both the launch and re-entry configurations.

The DFI provides an opportunity for researchers to use the Space Shuttle as a flight research vehicle. The results presented are part of the research activity which accomplishes the comparison of re-entry flight surface pressure to ground-based research data obtained computationally and in the wind tunnel.

The wind tunnel data were obtained in various ground research facilities using different models, and the computational data were obtained through solution of the three-dimensional Euler equations about a modified Orbiter geometry. The wind tunnel data range spans the re-entry Mach number range from hypersonic ($M_\infty = 10.0$) to subsonic ($M_\infty = 0.25$) for three different forward fuselage models (0.02-, 0.04-, and 0.10-scale). The computational data were obtained from the HALIS[1] (High Alpha Inviscid Solution) computer code for the continuum flow regime of the hypersonic Mach number range. The wind tunnel models were instrumented to duplicate locations of selected Orbiter surface DFI pressures. The computational data were also selected to match flight conditions and locations corresponding to these selected DFI pressure sensors. It is the purpose of this article to present the results of the evaluation and comparison of the forward fuselage pressure data obtained during the four OFT re-entries in terms of these ground-based pressure prediction techniques.

Space Shuttle Data System

During the OFT program, the Space Shuttle Orbiter has included various types of instrumentation and the data support equipment (the DFI system) necessary to obtain, telemeter, and record data at various sampling rates. The flight data obtained from the DFI are required for comparison with ground-based predictions.

Flight data used in this present study were obtained from the DFI surface pressure orifices located in the forward fuselage region. These orifices' pressure tubing penetrates the heat-resistant thermal protective system's (TPS) tiles, its bonding materials, and the Orbiter's aluminum skin, and is connected to absolute pressure transducers mounted to the Orbiter's internal structure. The transducer's 0 to 50-V analog output is digitized by an 8-bit Pulse Code Modulator (PCM) system. The DFI data system provides pressure data with a resolution of 0.39% of full scale. The transducer ranges are: 0 to 20 psi $\pm$0.078 psi, 0 to 15 psi $\pm$0.0586 psi, 0 to 1.04 psi $\pm$0.004 psi, and 0 to 0.52 psi $\pm$0.002 psi.‡

Presented as Paper 83-0119 at the AIAA 21st Aerospace Sciences Meeting, Reno, Nev., Jan. 10-13, 1983; submitted March 2, 1983; revision received Aug. 10, 1983. This paper is declared a work of the U.S. Government and therefore is in the public domain.

*Aerospace Engineer, Computational Methods Branch, High-Speed Aerodynamics Division.

†Aerospace Engineer, Aerothermodynamics Branch, Space Systems Division.

‡Note that references to DFI transducers are presented in English pressure units, while pressure data are plotted in SI units.

During STS-1 and STS-4 the DFI recorder malfunctioned, thereby restricting the data to that obtained from telemetry after blackout. This limited data to Mach numbers of 13 and below. Due to power constraints, a restricted amount of pressure data were available from STS-2. A complete set of data was, however, obtained during STS-3. The STS-3 data allowed a thorough analysis of the pressure data, as well as the behavior of the data system, and assisted in resolving discrepancies originally noticed between flight data and ground-based data. Where comparisons could be performed, however, pressure data from all flights displayed a high degree of consistency.

Calibration and Behavior of DFI Pressure Measurements

The initial STS-1 and -3 data analysis, comparing the flight data to the ground-based data, produced discrepancies which were attributed to transducer calibration and data system limitations. To resolve these discrepancies, an in-depth study of the behavior and calibration of the DFI transducers and the data system was initiated. This study has provided explanations for most of the discrepancies and is presented in this article.

The transducers each have a data range which varies from zero to a full-scale reading. Any reading below zero or above full scale is recorded by the data system as an off-scale low or high, respectively. Very few, if any, of the transducers indicate zero pressure on orbit. They indicate either a positive or negative value; this value is designated the bias. Any positive bias is registered on the data tape in the on-orbit phase of the mission and this positive number can be subtracted from the flight data. Any negative bias is recorded as an off-scale low and cannot be accurately determined by any known means. The reason for the inability to calculate the negative bias is illustrated in Fig. 1. The plot shows the behavior of two transducers, V07P9100 and V07P9451, at the same orifice location. V07P9100 is a 0-15 psi transducer with a known positive bias on-orbit of 0.22 psi. It reads that value until the Orbiter is low enough in the atmosphere for the pressure to be enough for the transducer to respond within the resolution of the data system. This response is a function of the resolution of the data system (0.0586 psi). V07P9451 is a 0-1.04 psi transducer with an unknown negative bias. Its pressure response is evidenced by a positive value several hundred seconds into the re-entry around 100 km in altitude (Fig. 1). Each transducer responds above its bias at a different time in the trajectory and there is no discernible response that can be attributed to a predictable flowfield. The random behavior in the very upper atmosphere prevents a computational prediction of when the transducers start to vary from the "flat" bias reading.

A group of transducers of the same type as the DFI exists and is part of the Shuttle Entry Air Data System (SEADS).[2] The SEADS is a new concept in air data systems capable of providing research quality air data from Mach 30 to the ground. The transducers for SEADS, which are identical to similarly ranged DFI transducers, have been rigorously calibrated to obtain an accuracy above that available from the current DFI system. The calibration of the SEADS transducers can provide generic type data applicable to the DFI transducers.

Results of the SEADS transducer calibrations indicate that transducer bias is temperature dependent. This dependency cannot be assessed for the DFI transducers because of a lack of temperature/time data for the DFI and therefore cannot be used in analyses of flight data and ground-based data differences. This introduces an uncertainty into the flight pressure data.

The conversion of the DFI transducer output from voltage to pressure in engineering units is of interest when assessing differences between flight data and ground-based data. While all of the DFI transducers were calibrated individually, a second-order polynomial curve fit was applied to the calibration curves to define a universal calibration curve for all transducers of the same pressure range. The use of this universal calibration curve can explain constant differences between flight data and ground-based data. It may also explain why some of the flight data curves match extremely well to the ground-based data whereas others do not.

Because of the limitations that exist in the DFI pressure data system, good agreement between flight data and ground-based data is said to exist when the ground-based data match the shapes of the flight data curves and are in the vicinity of the flight data.

Error Assessment of Flight Pressure Data

From the previous discussion it is clear that there are a number of uncertainties in the accuracy of the flight data that can manifest themselves into an error band about the flight data. The root mean square (rms) of the major contributing uncertainties will be used as an assessment of the accuracy of the flight data.

The manufacturer's specification for transducer accuracy is $\pm 5\%$ of full scale. Analyses of the more rigorous calibration data obtained from the SEADS transducers indicate an error due to scale factor (3σ) uncertainty of $\pm 2.4\%$ of reading. The accuracy determined from the SEADS calibration is used in the rms calculation of DFI pressure error.

The data word resolution for the 8-bit data system is calculated by the term below:

$$(\text{Full-scale reading})/(2^8 - 1)$$

The uncertainty in the pressure measurement due to temperature variation of the transducer has not been assessed for the DFI transducers. The results obtained during the calibration of the SEADS transducers indicate 2% of full-scale uncertainty due to temperature variation.

The root mean square of these three uncertainties is determined using the equation below and is plotted in Fig. 2 for $\Delta P/P$ vs P/P_{fs}. This equation is valid for transducers of all ranges.

$$\Delta P/P = \pm \{(0.02 P_{fs}/P)^2 + (0.024)^2 + [(1/255) \times (3/12) \times (P/P_{fs})]^2\}$$

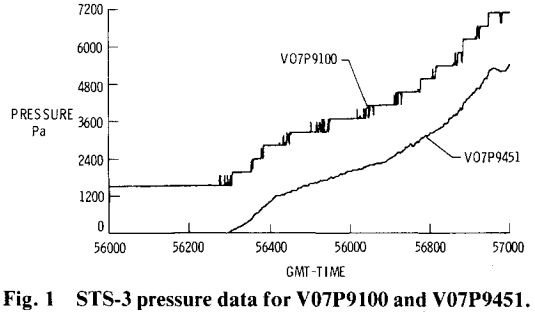

Fig. 1 STS-3 pressure data for V07P9100 and V07P9451.

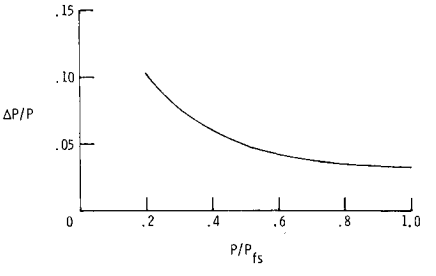

Fig. 2 Error assessment for DFI transducers.

In sensible regions of the atmosphere where P_i is above 0.2 psi, the uncertainty in the DFI pressure measurement for the 0-1.04 psi transducers is calculated to be less than 10%. For the 0-15 psi transducers, uncertainty is less than 10% for readings above 3 psi.

Description of HALIS Computer Code

The HALIS code is an explicit, three-dimensional, time-asymptotic Euler equation solver written to be processed on the CDC Cyber-203 computer.[1] The 203 uses vector processing and has large CPU storage capabilities. The HALIS solution used for these comparisons extends to a length of 650 in. back from the nose of the vehicle. Since the flow on the leeside of the Orbiter is dominated by viscous phenomena, the HALIS cannot properly model the leeside flowfield. Therefore, the complex leeside geometry has been modified, as shown in Fig. 3, to simplify the computational problem and allow a greater portion of the computer resources to be used for better resolution of the windward surface flowfield.

At angles of attack below 25 deg, the HALIS code is not cost effective when compared with spatial marching codes, which can handle the flowfield computations at the lower angles of attack. Thus, HALIS data are therefore presented only for the hypersonic Mach number range. Data shown plotted with the flight data are for perfect gas calculations, since the perfect gas results agree well with the flight data. HALIS can also compute real gas solutions and equilibrium air chemistry solutions, which have been shown to be within 5% of perfect gas calculations. Therefore, perfect gas solutions are presented for simplicity.

Wind Tunnel Models and Instrumentation

Three different scale models of the Orbiter's forward fuselage were used for the various wind tunnel tests. Portions of the Orbiter modeled are shown in Fig. 4. A 0.10-scale model was tested in the subsonic through supersonic Mach number range in the Arnold Engineering Development Center's 16T Tunnel and in the Ames Research Center Unitary Plan Wind Tunnel. This model was instrumented with 96 flush orifices corresponding to DFI, SEADS, and SEADS support locations.

A 0.04-scale model was tested in the supersonic through hypersonic Mach number range in the Langley Unitary Plan Wind Tunnel, Mach 10 Continuous Flow Hypersonic Tunnel (CFHT), and the 20-in. Mach 6 Tunnel. This model was instrumented with 72 flush orifices which also correspond to DFI, SEADS, and SEADS support locations.

A 0.02-scale model was tested at hypersonic Mach numbers in the Langley CFHT and 20-in. Mach 6 Tunnel. The model was instrumented with 36 flush orifices. Due to the small size of the model, only SEADS, DFI, and a few SEADS support orifices were duplicated.

Wind Tunnel Test Program

The three Orbiter forebody models tested provided a wide test matrix which produced an extensive across-the-speed-range data base; and although results presented here will include only those test conditions which closely match flight conditions, the remainder of the data are being used in the development of SEADS flight data reduction software.

The CFHT is a Mach 10 air facility currently operated only in the blowdown mode. It has a 0.79 m (31 in.) square test section.[3,4] The angle of attack (α) and angle of sideslip (β) ranges for the 0.04-scale model were -5 to 45 deg and -3 to 3 deg, respectively. For the 0.02-scale model, the ranges were -10 to 45 deg and -5 to 5 deg, respectively. Because of their higher quality, only the 0.02-scale model data are presented.

The 20 in. Mach 6 Tunnel is also operated in a blowdown mode with a test core of 0.406 m (16 in.) in the 0.508 m (20 in.) square test section. The angle-of-attack range was from 0 to 35 deg for the 0.04-scale model tests and -10 to 45 deg for the 0.02-scale model tests. The angle-of-sideslip range was from 0 to -4 deg for both tests. Again only the 0.02-scale model data are presented.

The two test sections in the Langley Unitary Plan Wind Tunnel operate in the continuous mode and each has its own Mach number range. The tunnel's nozzle is an asymmetrical sliding block allowing for variation in the test section Mach number. Data between Mach 2.3 and 4.65 were obtained on 0.04-scale model in the high-speed test section over the angle-of-attack range from -2.5 to 30 deg and the angle-of-sideslip range from -5 to 5 deg. Data between Mach 1.5 and 2.0 were obtained for the same α and β ranges in the low-speed test section.[3,4]

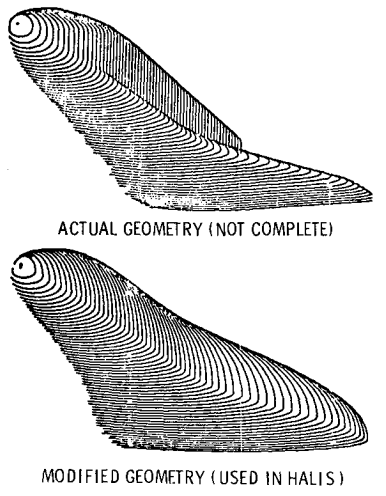

Fig. 3 Orbiter geometry—actual and modified.

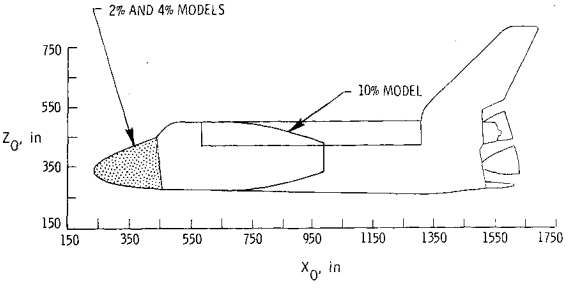

Fig. 4 Portions of the Orbiter modeled.

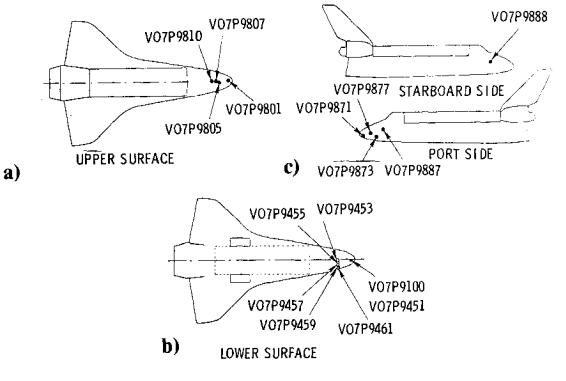

Fig. 5 a) Upper surface, b) lower surface, and c) port and starboard DFI transducers studied.

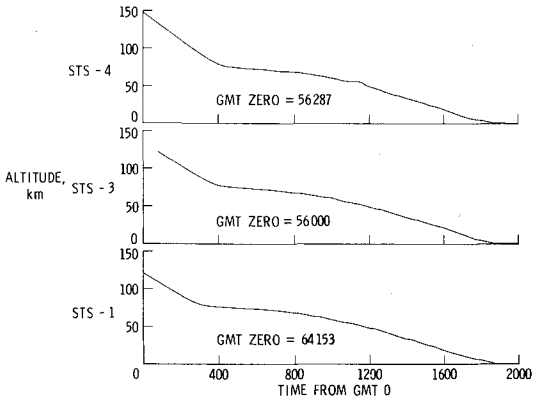

Fig. 6a Altitude vs time for STS-1, -3, and -4.

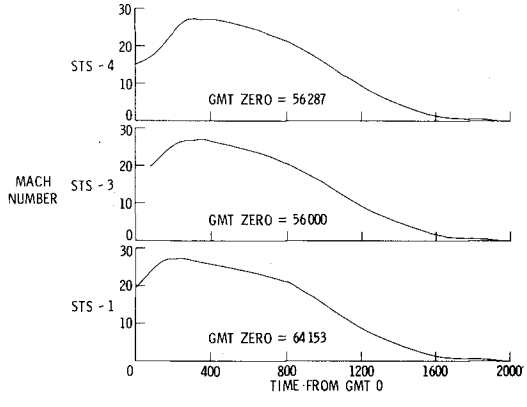

Fig. 6b Mach number vs time for STS-1, -3, and -4.

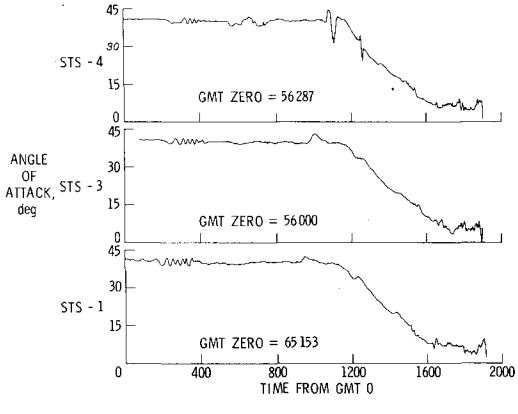

Fig. 6c Angle of attack vs time for STS-1, -3, and -4.

Tests completed in the Arnold Engineering Development Center's 16T Tunnel covered the Mach number range from 0.25 to 1.50. The 0.10-scale model was tested at angles of attack from -2 to 18 deg and angles of sideslip from -6 to 6 deg. The tunnel is a variable density, continuous flow tunnel capable of a Mach number range from 0.2 to 1.50 over a stagnation pressure range from 5745 Pa (0.83 psi) to 1.92×10^5 Pa (27.8 psi). The maximum stagnation pressure attainable depends on power availability. The tunnel's stagnation temperature can vary from 300 to 344 K, depending upon the cooling water temperature. Its test section is 4.88 m (16 ft) square and 12.12 m (40 ft) in length. The test section walls are 6% porous with 60 deg inclined holes.

Tests were completed in the Ames Research Center Unitary Plan Wind Tunnel in both the 9×7 ft and 8×7 ft test sections. The 0.10-scale model was tested over the angle-of-attack

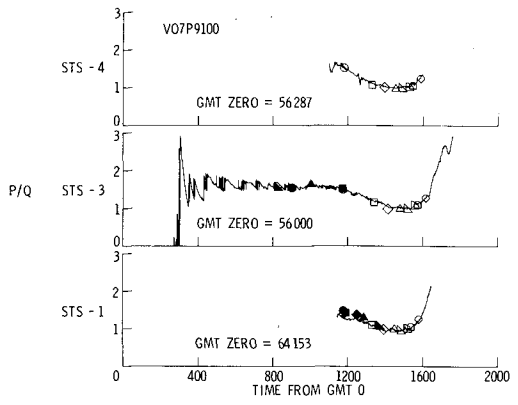

Fig. 7 Flight data comparisons with ground-based results for STS-1, -3, and -4, V07P9100.

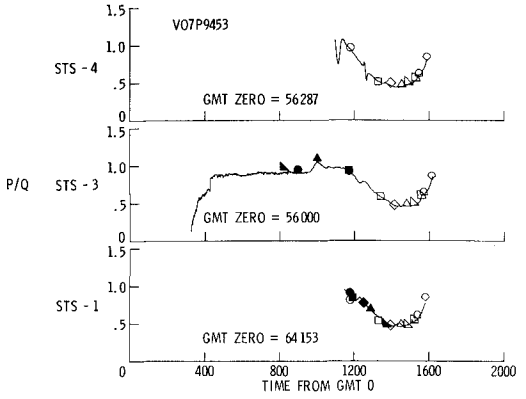

Fig. 8 Flight data comparisons with ground-based results for STS-1, -3, and -4, V07P9453.

range from -2 to 24 deg and the angle-of-sideslip range from -6 to 6 deg. The Mach number range in the 9×7 test section was 1.6 to 2.5 and in the 8×7 test section, 2.5 to 3.5. The tunnel is a closed-circuit, variable density, continuous flow tunnel.[4]

Analysis of Nondimensionalizing Parameter Freestream Dynamic Pressure

Ground-based data are nondimensionalized by freestream dynamic pressure, Q. Wind tunnel data are nondimensionalized by each tunnel's freestream dynamic pressure at the specific test conditions. Nondimensional computational data appear in the solution of the Euler equations as $P/\rho V^2$. P/Q is therefore twice the nondimensional pressure that is obtained from the HALIS code.

The flight data are also nondimensionalized by freestream dynamic pressure which may be calculated by different methods. The decision of which calculation of dynamic pressure to select, based on analysis of the available calculations, was lengthy and covered the first three flights. A combination of two methods appears to give the most reasonable solution. The use of comparisons with ground-based data assisted in making this decision.

For navigation purposes, an estimate of Q is derived, used in the general purpose computer (GPC), and included in the recorded data. This estimate, NAVQ, was used to nondimensionalize STS-1 data. Above Mach 3.5, NAVQ is calculated from the Orbiter's drag acceleration, drag coefficient, and surface area. Both drag coefficient and surface area are a function of angle of attack, with drag coefficient coming from the wind tunnel data base.[5] Below Mach 3.5, side probes are deployed to receive air data for parameter calculations. The specification for uncertainty for NAVQ is

±15% of reading. The data plots for STS-1 give reasonable agreement among data sources, indicating the NAVQ solution for STS-1 below Mach 12 is a reasonable solution.

Data obtained during STS-3 covered the entire re-entry trajectory. The NAVQ solution was again used initially as the nondimensionalized parameter. Analysis of the comparison plots indicated problems with agreement between the high hypersonic calculations from the HALIS code (Mach 10-20) and the nondimensionalized flight data.

Another solution for dynamic pressure was obtained from Langley's Best Estimate Trajectory (BET). This trajectory reconstruction process is discussed by Compton, et al.[6] The calculation of dynamic pressure uses velocity information integrated from the accelerations the Orbiter experienced during re-entry and atmospheric information obtained from several sources. Independent atmospheric information is processed by the Langley Atmospheric Information Retrieval System (LAIRS).[7] The use of BETQ generally improved agreement among data sources, but some regions in the very upper portion of the trajectory appeared to be unreliable when compared with ground-based data. Investigations of the meteorological data received for the LAIRS system indicated possible anomalies which could not be resolved.

A third source for the dynamic pressure calculations was obtained from a solution based on the algorithm being developed for analysis of the data to be received from SEADS.[8] By using modified Newtonian theory, certain of the DFI, and altitude data from the BET, freestream dynamic pressure was derived from measurements obtained during re-entry from two of the pressure transducers, specifically, V07P9451 and V07P9100. The SEADS calculation has been analyzed and compared to other sources of dynamic pressure calculation with the conclusion that the SEADS method of calculating Q is most applicable in the region from 74 km (245,000 ft) to 56 km (185,000 ft) in altitude. The SEADS Q was then combined with the BETQ, with the SEADSQ replacing the BETQ in the region from 74 to 56 km. This combination of the two solutions was used to nondimensionalize the STS-3 flight data and is that shown in the data plots for STS-3. This combined Q gives the best agreement among data sources from the solutions mentioned here.

Results and Discussion

Wind tunnel data have been obtained for 16 orifices corresponding to forward fuselage DFI pressure orifices. Data from seven orifices are discussed in detail here. Comparisons of the flight data from three of these orifices are made with computational data obtained from the HALIS code. Symbol identification is given in Table 1.

The locations on the Orbiter of the 16 orifices are shown in Figs. 5a-c. Flight conditions for STS-1-3, and 4 are given in Figs. 6a-c. Information from the three flights is aligned based on the location of Mach 10 for STS-3 such that Mach 10 data are located at the same point on the time axis for each flight. Extrapolation back gives the Greenwich mean time (GMT) zero noted on each plot. Figure 6a gives the altitude vs time for all three flights; Fig. 6b, the Mach number vs time; and Fig. 6c, the angle of attack vs time.

Data from the pressure port nearest the nose on the lower surface are shown in Fig. 7. This orifice has two transducers colocated at the same port with two different pressure ranges. The 0-15 psi transducer (V07P9100) data are shown. For regions in the upper atmosphere, where pressure levels are extremely low, the transducer output appears extremely noisy, but is in actuality only a function of the resolution of the data system. Data below Mach 10 are much smoother as is evidenced in all three plots. Because of this transducer's data range, flight data are available to landing. The data plots do not, however, include data for which the nondimensionalizing parameter (Q) is less than 0.007 psi. Both the wind tunnel and the HALIS data for this location match the flight data well within the error band of the flight data. Where angle-of-attack excursions (aeromaneuvers) are noted in the flight pressure data, corresponding ground-based information gives similar nondimensional pressure levels. This can be noted in this and other figures for Mach 15 (HALIS) during STS-3, and Mach 3.5 (wind tunnel) for STS-1. The two pressure excursions noted just after blackout and around Mach 8 during STS-4 are documented aeromaneuvers which are noted in all the flight data plots for STS-4.

Figures 8 and 9 show comparisons of flight data for the three flights with ground-based data for two transducers of an array of pressure orifices starting at the centerline of the Orbiter and extending out to the chine. This meridional array is located 3.25 m (128 in.) back from the Orbiter's nose. All of these DFI ports have 0-1.04 psi transducers which provide good data resolution. All the ground-based data are well

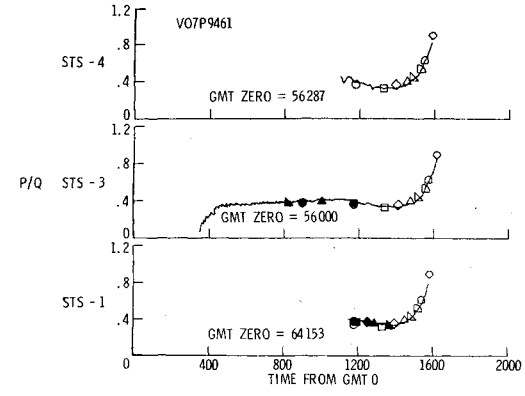

Fig. 9 Flight data comparisons with ground-based results for STS-1,-3, and -4, V07P9461.

Table 1 Symbol identification for data plots

Flight data, all plots		
HALIS, STS-1 Mach no.	HALIS, STS-3 Mach no.	Wind tunnel all plots Mach no.
●	◣ 20	○ 10
■ 9	● 18	□ 6
◆ 7.5	▲ 15.3	◇ 4.63
▲ 6.5	■ 10	△ 3.5
◣ 5		◺ 2.96
		◺ 2.3
		⌂ 2
		◇ 0.5

Table 2 Symbol identification for Fig. 14

	Flight data	Mach no.
♂	AEDC	0.25
⌂	↓	0.4
◊	↓	0.6
◇	↓	0.8
⌂	↓	0.95
◺	↓	1.1
◺	↓	1.15
△	↓	1.2
◇	↓	1.3
□	↓	1.4
○	↓	1.5
■	LaRC	1.5
◈	ARC 9×7	1.6
⊞	↓	1.8
⊕	↓	2.0
●	LaRC	2.0

within the flight data error band. Saturation of these transducers is around Mach 1.5 for each flight. This array of transducers is an excellent example of the calibration/bias uncertainties. V07P9453 and V07P9461 both have unknown negative biases. For V07P9453, the flight data are consistently lower than the ground-based data for all three flights, indicating that a bias correction could result in better agreement among data sources. The data obtained for V07P9461 are slightly higher than ground-based data. A bias correction would not help the agreement. This is an indication that the bias may be only slightly negative and may be a function of temperature. This slight disagreement could also be caused by the use of the "universal" calibration curve.

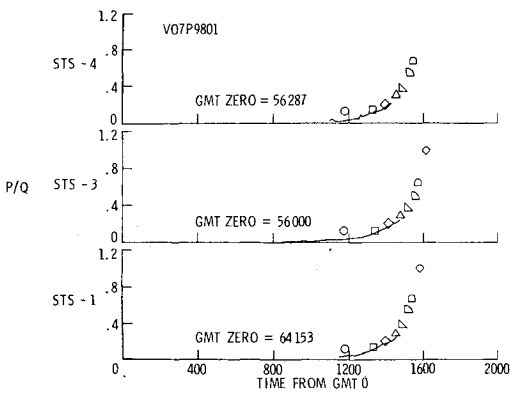

Fig. 10 Flight data comparisons with ground-based results for STS-1,-3, and -4, V07P9801.

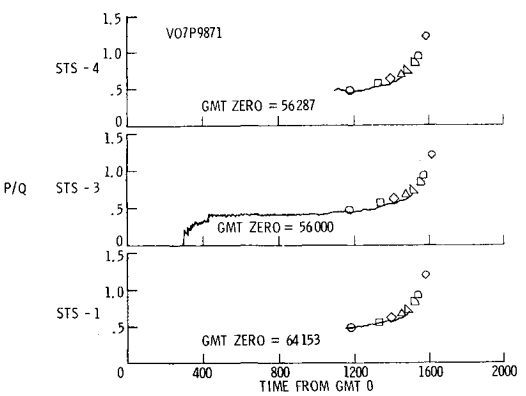

Fig. 11 Flight data comparisons with ground-based results for STS-1,-3, and -4, V07P9871.

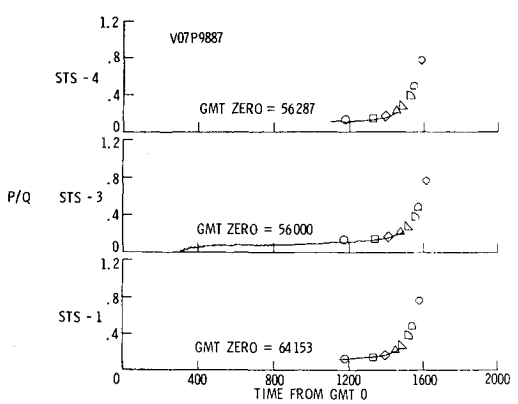

Fig. 12 Flight data comparisons with ground-based results for STS-1,-3, and -4, V07P9887.

Data obtained from the upper surface DFI in the forward fuselage region are extremely restrictive, since most of the transducers are of extremely low range (0-0.1 psi). This region is also dominated by viscous phenomena, making solutions from the HALIS code invalid in this region. For these reasons, upper surface data presented will be limited to one port location. The upper surface data shown in Fig. 10 are for the transducer V07P9801. This transducer has an unknown negative bias, which, if it were known and added to the data, would help agreement with the ground data. This transducer saturates around Mach 4 in all three flights giving very restrictive comparisons with the wind tunnel data. A temperature-dependent bias may be the source of differences between flight and wind tunnel data, since the differences are not constant.

On the port side of the Orbiter, data are shown for V07P9871 in Fig. 11. V07P9871 has a known on-orbit positive bias. Flight data for V07P9871 are slightly lower than the wind tunnel data by a fairly constant amount. Differences could be attributed to the calibration procedure.

Data are shown in Figs. 12 and 13 for a pair of transducers located on the port and starboard sides of the Orbiter at the same X, Z locations. V07P9887 has a known on-orbit positive bias and V07P9888 has an unknown negative bias. Data comparisons between flight and wind tunnel are very good. A slightly negative bias for V07P9888, if known and applied to the flight data, could help the agreement. Symmetry of the Orbiter is apparent when comparing the two. This result demonstrates that the trajectory displays little sideslip relative to the air mass.

Flight data for the 0-15 psi transducer V07P9100 are shown in Fig. 14 for the Mach number range of 2.0 and below. These data are nondimensionalized by P_{t_2} since Q becomes small

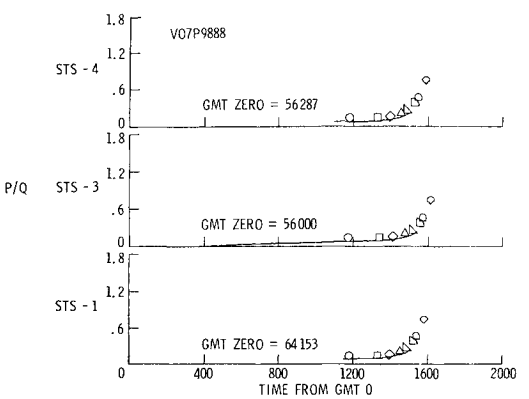

Fig. 13 Flight data comparisons with ground-based results for STS-1,-3, and -4, V07P9888.

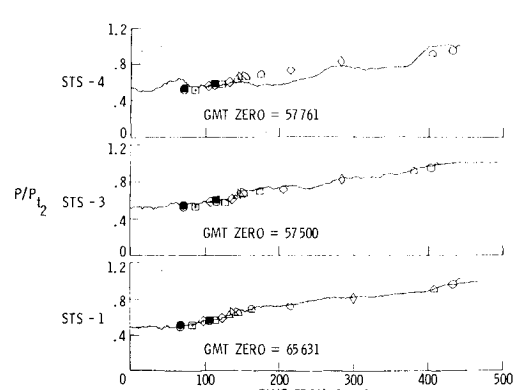

Fig. 14 Comparisons between flight data and wind tunnel data at Mach 2.0 and below, V07P9100.

compared to the surface pressures. A P/Q plot in this data range would require a much expanded ordinate axis which would restrict detailed analyses. The P_{t_2} used was obtained from the BET.

Wind tunnel data from the Unitary Plan Wind Tunnels at Langley (0.04-scale model) and Ames (0.10-scale model) Research Centers and Arnold Engineering Development Center's 16T Tunnel (0.10-scale model) are plotted in the figure for all three flights. Symbol identification for Fig. 14 is given in Table 2. The wind tunnel data match the flight data well within the error band established for the flight data. The wind tunnel data on these plots are nondimensionalized by the wind tunnel's P_{t_2}. Unlike previous data plots in the supersonic/hypersonic Mach number range, where flight data is suspected to have calibration and/or bias uncertainties, data in this region for this transducer are least likely to be affected by temperature, and bias uncertainties would become small compared to the magnitude of the pressure reading. Data system uncertainties are also small compared to the magnitude of the pressure reading.

The only notable discrepancy in the figure is on the STS-4 plot. Mach number and angle of attack information obtained from the BET for all three flights shows very few differences in the transonic region ($M_\infty = 1.5$ to 0.8) among the three flights. Since flight/wind tunnel data agreement is good for the other two flights, the slight drop in nondimensional pressure in this region may be an indication of uncertainty arising from atmospheric information. The P_{t_2} used to nondimensionalize the flight data are obtained using perfect gas relations, Mach number (from the BET), and freestream static pressure. The use of this calculation has helped to provide good agreement between ground and flight data and is therefore used in this set of plots. The uncertainties noted for STS-4 can be analyzed with the other two flights and with the wind tunnel data to determine that the "dip" in the curve is more likely the result of atmospheric information uncertainties rather than Orbiter performance uncertainties.

Conclusions

Pressure data obtained from the Space Shuttle Orbiter's Development Flight Instrumentation in the forward fuselage region during the STS-1 through STS-4 re-entries have been compared to wind tunnel and computational data. Ground-based data across the hypersonic/subsonic Mach number range matched the flight data within the uncertainty calculated for the DFI system. An analysis of the calibration procedures associated with in-flight behavior of the transducers has provided a better understanding of the DFI system and explained differences between the ground-based and the flight data. A discussion of the various methods which determine freestream dynamic pressure during the re-entry has resulted in a good Q selection for nondimensionalizing the flight pressure data. This selection of Q provides the best agreement between ground-based and flight data. These comparisons between ground-based and flight data, which were completed in support of the development of the SEADS software, have helped to verify the analytical method for SEADS data reduction, which includes an extensive wind tunnel data base.

As a result of the analyses presented, certain conclusions are noted here. Agreement between ground-based and flight data, although good, is dependent upon resolution and quality of the flight data system and preflight calibration of the transducers. The analysis indicates that more orifices of different ranges (more applicable to the re-entry environment) are needed onboard the Orbiter for accurate pressure modeling. An accurate pressure model of the Orbiter in flight is needed for aerodynamic force and moment calculations. Both the wind tunnel tests completed on the forward fuselage models and the HALIS computer program predict in-flight forward fuselage pressure distributions well. Both ground-based techniques can be used confidently, although HALIS data are currently restricted to the windward surface. This constraint is due to the fact that HALIS is an inviscid code, whereas the Orbiter's leeside is dominated by viscous effects. The accurate determination of freestream dynamic pressure is critical. This is one justification for an across-the-speed-range air data system for the Orbiter. Finally, the algorithm developed for SEADS to derive freestream properties from the forward fuselage pressure distribution, which is based on modifications to Newtonian theory, has been demonstrated with the present data and appears to provide an accurate estimate of freestream dynamic pressure.

References

[1] Weilmuenster, K. J. and Hamilton, H. H., "A Method for Computation of Inviscid Three-Dimensional Flow Over Blunt Bodies Having Large Embedded Subsonic Regions," AIAA Paper 81-1203, June 1981.

[2] Siemers, P. M. III, "Shuttle Entry Air Data System," presented at the 1978 Air Data Systems Conference, Colorado Springs, Colo., May 3, 1978.

[3] Shafer, W. T. Jr., "Characteristics of Major Active Wind Tunnels at the Langley Research Center," NASA TMX-1130, July 1965.

[4] Pirrelo, C. T., Hardin, R. D., Heckart, M. V., and Brown, K. R., "An Inventory of Aeronautical Ground Research Facilities," Vol. I, Wind Tunnels, NASA CR-1874, Nov. 1971.

[5] *Aerodynamic Design Data Book,* SD72-SH-0060, Vol. IL. WBS No. 1.2.2.1.1, IRD No. Se640T2, Rockwell International, Oct. 1978.

[6] Compton, H. R., Findlay, J. T., Kelly, G. M., and Heck, M. L., "Shuttle (STS-1) Entry Trajectory Reconstruction," AIAA Paper 81-2459, Nov. 1981.

[7] Price, J. M., "Atmospheric Definition for Shuttle Aerothermodynamic Investigations," *Journal of Spacecraft and Rockets,* Vol. 20, March/April 1983, pp. 133-140.

[8] Pruett, C. D., Wolf, H., Siemers, P. M. III, and Heck, M. L., "An Innovative Air Data System for the Space Shuttle Orbiter: Data Analysis Techniques," AIAA Paper 81-2455, Nov. 1981.